extracts (10 μg) were separated by SDS–polyacrylamide gel electrophoresis (8% gel for the SERCA1 immunoblot and 4% gel for the IP_3R blot). After electrophoresis, the proteins were transferred to nitrocellulose. The avian SERCA1 immunoblot was probed with a mAb extract (mouse antibody to chicken) diluted 1:1500. The IP_3R immunoblot was probed with a polyclonal antibody (rabbit antibody to mouse) diluted 1:2000. The IP_3R immunoblot is negative when incubated with preimmune serum (P. Camacho and J. D. Lechleiter, unpublished data). After incubation with primary antibody, exposure to a secondary alkaline phosphatase (AP)–conjugated immunoglobulin G (IgG) was done according to the manufacturer's instructions (goat antibody to mouse IgG for SERCA1 and goat antibody to rabbit IgG for the IP_3R, both from Promega, Madison, WI). Colorimetric detection was obtained within 20 min of exposure to the NET/BCIP color substrates (ProtoBlot protein immunoblot AP system, Promega).

19. G. A. Mignery, T. C. Südhof, K. Takei, P. De Camilli, *Nature* **342**, 192 (1989); T. Furuichi *et al.*, *ibid.*, p. 32; J. B. Parys *et al.*, *J. Biol. Chem.* **267**, 18776 (1992).
20. E. Carafoli, *Annu. Rev. Biochem.* **56**, 395 (1987).
21. S. Girard, A. Luckhoff, J. Lechleiter, J. Sneyd, D. Clapham, *Biophys. J.* **61**, 509 (1992).
22. C. Brandl, N. Green, B. Korczak, D. H. MacLennan, *Cell* **44**, 597 (1986); C. Brandl, S. deLeon, D. Martin, D. H. MacLennan, *J. Biol. Chem.* **262**, 3768 (1987); A. Gunteski-Hamblin, J. Greeb, J. Shull, *ibid.* **263**, 15032 (1988); J. Lytton and D. H. MacLennan, *ibid.*, p. 15024.
23. We thank K. Takeyasu for the avian SERCA1 cDNA and mAb, P. DeCamilli for the polyclonal antibody to the IP_3R, D. Castle for rat brain membrane extracts, and H. Kutchai, E. Nasi, and E. Peralta for their critical reading of the manuscript.

3 November 1992; accepted 12 January 1993

Acceleration of Intracellular Calcium Waves in *Xenopus* Oocytes by Calcium Influx

Steven Girard and David Clapham*

Many cell membrane receptors stimulate the phosphoinositide (PI) cycle, which produces complex intracellular calcium signals that regulate diverse processes such as secretion and transcription. A major messenger of this cycle, inositol 1,4,5-trisphosphate (IP_3), stimulates its receptor channel on the endoplasmic reticulum to release calcium into the cytosol. Activation of the PI cycle also induces calcium influx, which refills the intracellular calcium stores. Confocal microscopy was used to show that receptor-activated calcium influx, enhanced by hyperpolarization, modulates the frequency and velocity of IP_3-dependent calcium waves in *Xenopus laevis* oocytes. These results demonstrate that transmembrane voltage and calcium influx pathways may regulate spatial and temporal patterns of IP_3-dependent calcium release.

Propagating waves of elevated intracellular Ca^{2+} may be triggered in *Xenopus* oocytes by the activation of muscarinic receptors or by the microinjection of either guanosine-5′-O-(3-triphosphate) or IP_3 isomers (*1–4*). Calcium release from IP_3-sensitive intracellular stores (*5*) is necessary for both initiation and propagation of these waves (*2–4*). IP_3-dependent Ca^{2+} waves persist in the oocyte for up to 30 min in the absence of extracellular Ca^{2+} (*2, 3*). We used confocal fluorescence microscopy with conventional two-electrode voltage clamp to study Ca^{2+} influx and its influence on IP_3-dependent Ca^{2+} waves (*6–9*). Fluorescence from Calcium Green was recorded from superficial optical sections (628 by 419 μm) within ~30 μm of the plasma membrane (*10*).

To investigate the effects of Ca^{2+} influx on receptor-induced Ca^{2+} transients, we applied acetylcholine (ACh) to oocytes that expressed human m3 muscarinic acetylcholine receptors (m3AChRs) (Fig. 1). Saturating concentrations of ACh (50 μM) triggered Ca^{2+} release from intracellular stores, which resulted in an increased concentration of Ca^{2+} that slowly decayed to base line over ~10 min (Fig. 1, A to D) (*11*). Hyperpolarization in the presence of 2.5 mM extracellular Ca^{2+} induced Ca^{2+} influx up to ~13 min after the application of atropine (200 μM) (*12*). In contrast to the generalized Ca^{2+} transient induced by high concentrations of ACh, submaximal stimulation (0.2 to 1 μM ACh) triggered regenerative Ca^{2+} waves (Fig. 1, E to G) that appear as streaks of increased fluorescence in a volume projection (Fig. 1F). The Ca^{2+} waves and Ca^{2+}-activated Cl^- current ($I_{Cl,Ca}$) oscillations stopped within seconds after the application of atropine (200 μM at 550 s), whereas the hyperpolarization-induced influx of extracellular Ca^{2+} persisted for more than 7 min (Fig. 1F) (*13*). Unstimulated cells showed no Ca^{2+} influx with hyperpolarization (n = 5). Because Ca^{2+} influx persisted for minutes after the Ca^{2+} waves were abolished, we speculate that other second messenger mechanisms triggered Ca^{2+} entry or that the concentrations of IP_3 were sufficient to bind to a receptor site that caused Ca^{2+} influx (*14*). These results also show that Ca^{2+} influx caused a generalized increase in Ca^{2+} but did not itself cause regenerative waves.

We examined the influence of Ca^{2+} influx on Ca^{2+} waves induced by injection of a nonmetabolizable IP_3 analog, inositol 1,4,5-trisphosphorothioate (IP_3S_3) (*15*). In the absence of extracellular Ca^{2+}, the waves induced by IP_3S_3 (5 μM) had a period, or interval between transients, that slowly increased over time (Fig. 2, A to D). The Ca^{2+} wave velocity was independent of membrane potential in ten experiments conducted in the absence of extracellular Ca^{2+} (Fig. 2E), which indicates that the kinetics of the IP_3 receptor (IP_3R) channel are not directly altered by changes in membrane potential.

In the presence of 2.5 mM extracellular Ca^{2+}, hyperpolarization triggered Ca^{2+} influx in 35 of 46 oocytes injected with IP_3S_3 (5 μM) (*16*), and no Ca^{2+} influx was observed in noninjected oocytes under similar conditions (n = 10). The entry of extracellular Ca^{2+} reversibly affected the frequency and velocity of Ca^{2+} waves triggered by IP_3S_3 (5 μM) (Fig. 3), an effect that was blocked by extracellular La^{3+} (1 mM) (*17*). In one oocyte, the wave velocity varied with the holding potential after the concentration of extracellular Ca^{2+} was raised to 2.5 mM (Fig. 3D). The mean velocity increased from 25.1 ± 0.8 μm s^{-1} (n = 5) to 33 ± 2 μm s^{-1} (n = 3) during a second hyperpolarizing pulse from −15 to −70 mV with 2.5 mM extracellular Ca^{2+}, and after depolarization to −15 mV the velocity returned to 25.4 ± 0.9 μm s^{-1} (n = 2). The wave velocity in this experiment ranged from 19 to 37 μm s^{-1} and was correlated with the local base line fluorescence before each wave (Fig. 3F). These data suggest that the influx of extracellular Ca^{2+} may alter the propagation of IP_3-dependent Ca^{2+} waves by increasing the basal Ca^{2+} concentration. This modulation of the velocity of Ca^{2+} waves was best observed with large changes in the membrane potential (~70 mV), which correlate to larger Ca^{2+} influxes.

Depolarization, which reduces the driving force for Ca^{2+} entry into the cell, decreased the resting concentration of Ca^{2+} and increased the period between successive wave fronts (Fig. 4, A to H). These alterations in wave frequency were reversible (Fig. 1, E and F, and Figs. 3 and 4). Calcium Green signals from 33-μm square regions (Fig. 4A) showed that the frequency of Ca^{2+} waves increased from 1.8 ± 0.2 min^{-1} at 0 mV to 5.2 ± 1.4 min^{-1} at −50 mV (mean ± SEM; n = 9). A comparison of the local Calcium Green signal from one region (Fig. 4G) and the signal averaged over the entire slice (Fig. 4H) showed that averaging over the entire section obscures the high frequency waves. Regions capable of initiating waves at −50 mV but not at more depolarized potentials appear as short segments of fluorescence in the volume projection (Fig. 4E), which suggests that different regions have unique threshold cytosolic Ca^{2+} concentrations that must be reached before waves are initiated. This

Department of Pharmacology, Mayo Foundation, Rochester, MN 55905.

*To whom correspondence should be addressed.

recruitment of initiation foci was, in part, responsible for the increase in frequency. Strong hyperpolarization in some oocytes arrested the IP_3S_3-induced waves (Fig. 4, I to L), which demonstrates that increases in cytosolic Ca^{2+} concentration over a critical level reversibly inhibit waves (*18*).

Calcium waves depend on the regenerative production of a diffusible molecule that triggers Ca^{2+} release from adjacent IP_3-sensitive stores. Because both IP_3 and cytosolic Ca^{2+} influence Ca^{2+} release at the oocyte IP_3R channel (*19*), either could function as this propagating signal. IP_3 diffuses more rapidly than Ca^{2+} in cytosolic extracts from *Xenopus* oocytes (*20*), but our experiments with high concentrations of IP_3S_3 (100 μM) indicate that oscillations in the amounts of IP_3 are not required for Ca^{2+} waves (*21*). Rather, these data suggest that activation of m3AChRs leads to a steady increase in IP_3 and that Ca^{2+} released from one store propagates through the cytoplasm and triggers release from neighboring stores. Here, we have demonstrated that Ca^{2+} entry from the extracellular space can modulate the frequency and propagation rates of this dynamic process. The modulatory role for Ca^{2+} influx provides control and allows diversity of signaling end points for the otherwise convergent phosphoinositide cascade. The spatial and temporal regulation of intracellular Ca^{2+} waves by Ca^{2+} influx means that the combination of membrane voltage and receptor-activated Ca^{2+} influx pathways greatly expands the range of signal transduction control for Ca^{2+}-dependent events ranging from transcription to secretion.

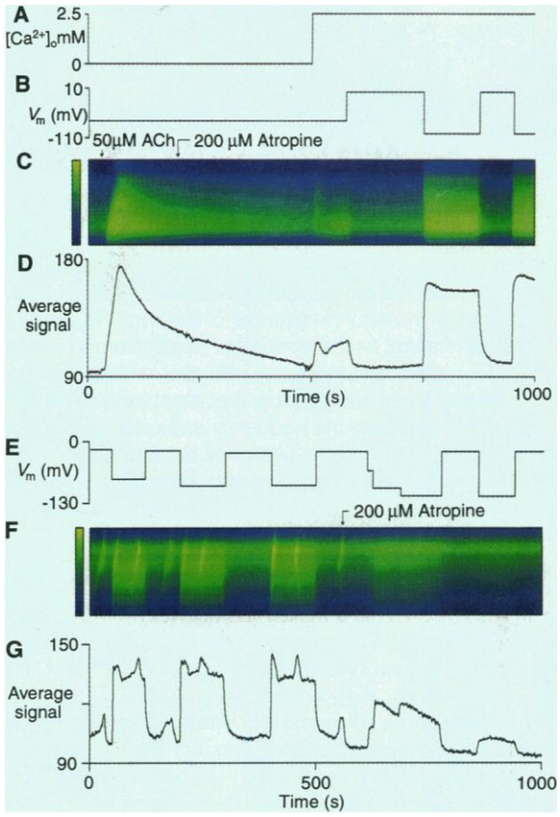

Fig. 1. Demonstration of m3AChR-activated Ca^{2+} influx. In (A) to (D), a *Xenopus* oocyte that expressed m3AChRs and was injected with Calcium Green (12 μM) (*22*) 20 min before study was stimulated with ACh (50 μM) 20 s into the experiment and then treated with atropine (200 μM) at 200 s. The concentration of extracellular Ca^{2+} and the membrane potential were manipulated to study Ca^{2+} influx after the application of antagonist. To follow the spatiotemporal transients of intracellular Ca^{2+}, we scanned a single 628 by 419 μm optical section (1 Hz) for 1000 s and the digital images (192 by 128 pixels) were stored with 256 gray scale values. The confocal section covered ~8% of the oocyte's surface area. (**A**) Extracellular Ca^{2+} concentration ($[Ca^{2+}]_o$). (**B**) Membrane potential (V_m) was clamped at −70, 0, −100, 0, and −100 mV. (**C**) ANALYZE software (*8*) was used to stack the confocal images into a volume (192 by 128 by 1000 pixels) of digital data. This panel (192 by 1000 pixels) represents a two-dimensional projection (view) of this volume, shown with time increasing to the right. The gray scale values of this panel represent the fluorescence intensity along the reader's line of sight into the volume. A pseudocolor scale bar for fluorescence intensity is next to (C); gray scales of 0 are blue, and gray scales of 255 are yellow-green (*22*). (**D**) The average Calcium Green signal of the 24,576 pixels in each confocal image (192 by 128 pixels) was calculated, and this average was displayed with increasing time. In (E) to (G), an m3AChR-expressing oocyte was stimulated with ACh (1 μM) ~1 min before imaging. The membrane potential was manipulated in the presence of 2.5 mM extracellular Ca^{2+} to study the effect of influx before and after the application of atropine (200 μM) at 550 s [denoted by the arrow on (F)]. (**E**) Membrane potential (V_m) was pulsed from the holding potential of −20 mV to −80, −95, −95, (−60, −100, −115), and −115 mV. (**F**) Volume projection of the 1000 images displayed with time increasing to the right. Propagating Ca^{2+} waves appear as arcs of increased signal above a base line fluorescence. Preliminary experiments with indo-1 suggest that the amplitude of a typical Ca^{2+} wave is greater than 300 nM. (**G**) Average Calcium Green signal in the confocal section.

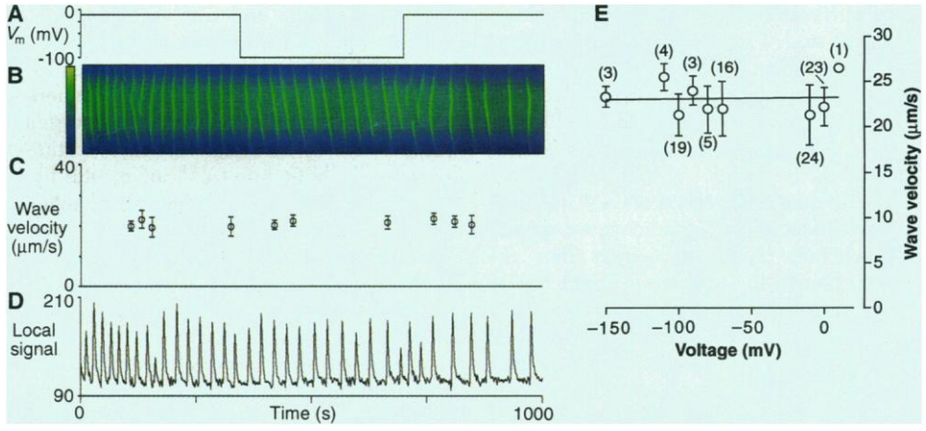

Fig. 2. Periodic Ca^{2+} waves triggered by IP_3S_3 propagate at a steady velocity in the absence of extracellular Ca^{2+}. This oocyte was injected with IP_3S_3 (5 μM) ~8 min before imaging under voltage clamp in the absence of extracellular Ca^{2+}. (**A**) Membrane potential (V_m) was pulsed to −100 mV from a holding potential of 0 mV. (**B**) Volume projection of the 1000 images displayed with time increasing to the right. (**C**) Velocities of Ca^{2+} waves ± SD. Planar Ca^{2+} waves were studied if they sustained propagation for more than 4 s in a given direction and if they did not interact with other waves. A vector in the direction of propagation was constructed by eye with ANALYZE software (*8*), and the position of the wave front along this line was recorded for successive images. The slope of a linear best fit of the wave front position expressed as a function of time gave the wave velocity and an error of this estimate. (**D**) Average Calcium Green signal in a 33-μm square region centered in the confocal section. (**E**) Summary of 97 wave velocities (mean of data at each voltage ± SD) measured in ten oocytes at various holding potentials in the absence of extracellular Ca^{2+}. The number of waves observed at each voltage is given in parentheses.

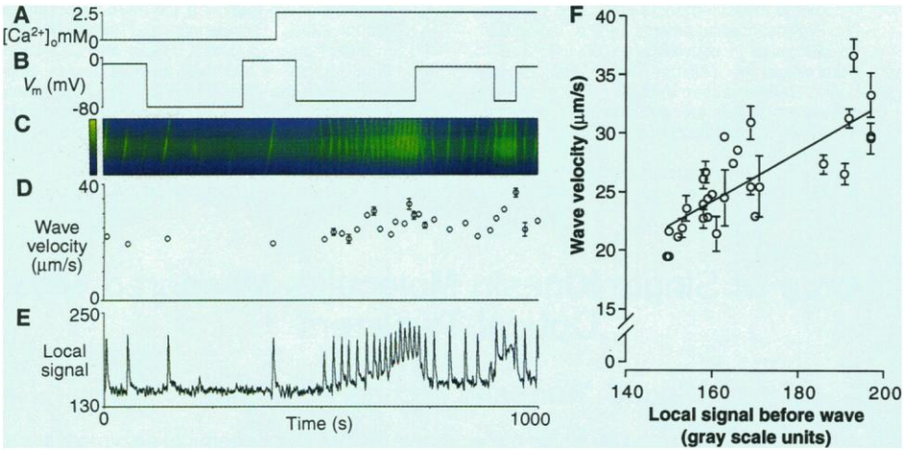

Fig. 3. Increased frequency and velocity of IP_3S_3-induced Ca^{2+} waves after Ca^{2+} influx. The oocyte was injected with IP_3S_3 (5 μM) ~10 min before imaging. (**A**) Extracellular Ca^{2+} concentration ($[Ca^{2+}]_o$). (**B**) Membrane potential (V_m) was clamped at −10, −80, −5, −70, −15, −70, and −15 mV. (**C**) Volume projection of the 1000 images displayed with time increasing to the right. (**D**) Velocities of Ca^{2+} waves ± SEM. Where error bars are not shown, the least squares estimate had a standard error less than the width of the symbol. (**E**) Average Calcium Green signal in a 33-μm square region centered in the confocal section. (**F**) Wave velocity as a function of the local resting signal averaged for the 4 s immediately before the initiation of each wave (r = 0.8).

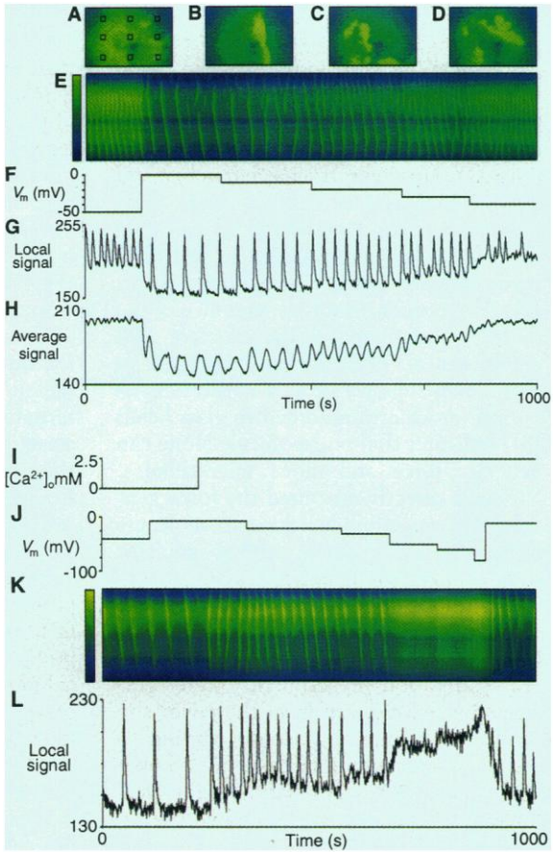

Fig. 4. Recruitment of new initiation foci and increased frequency of IP_3-induced Ca^{2+} waves after hyperpolarization. In (A) to (H), an oocyte was injected with IP_3S_3 (5 μM) ~15 min before imaging in the presence of 2.5 mM extracellular Ca^{2+}. (**A** to **D**) Confocal images of active Ca^{2+} waves at 1, 179, 570, and 828 s, respectively. Nine local (33-μm square) regions are shown in (A). (**E**) Volume projection of the 1000 images displayed with time increasing to the right. (**F**) Membrane potential (V_m) was clamped at −50, 0, −10, −20, −30, and −40 mV. (**G**) Average Calcium Green signal in a 33-μm square region [right square of the middle row in (A)]. (**H**) Average Calcium Green signal in the confocal section. In (I) to (L), an oocyte was injected with IP_3S_3 (5 μM) ~8 min before experimentation. (**I**) Extracellular Ca^{2+} concentration ($[Ca^{2+}]_o$). (**J**) Membrane potential (V_m) was clamped at −40, −7, −20, −30, −50, −60, −80, and −10 mV. (**K**) Volume projection of the 1000 images displayed with time increasing to the right. (**L**) Average Calcium Green signal in a 33-μm square region centered in the confocal section.

REFERENCES AND NOTES

1. G. Brooker, T. Seki, D. Croll, C. Wahlestedt, *Proc. Natl. Acad. Sci. U.S.A.* **87**, 2813 (1990).
2. J. Lechleiter, S. Girard, E. Peralta, D. E. Clapham, *Science* **252**, 123 (1991).
3. J. Lechleiter and D. E. Clapham, *Cell* **69**, 283 (1992).
4. S. DeLisle and M. J. Welsh, *J. Biol. Chem.* **267**, 7963 (1992).
5. L. E. Hokin, *Annu. Rev. Biochem.* **54**, 205 (1985); M. J. Berridge, *J. Biol. Chem.* **265**, 9583 (1990); ———, P. H. Cobbold, K. S. R. Cuthbertson, *Philos. Trans. R. Soc. London Ser. B* **320**, 325 (1988); M. J. Berridge and R. F. Irvine, *Nature* **341**, 197 (1989); R. W. Tsien and R. Y. Tsien, *Annu. Rev. Cell Biol.* **6**, 715 (1990); Y. Tsunoda, *New Biol.* **3**, 1, 3 (1991); A. P. Thomas, D. C. Renard, T. A. Rooney, *Cell Calcium* **12**, 111 (1991); T. Meyer and L. Stryer, *Annu. Rev. Biophys. Biophys. Chem.* **20**, 153 (1991); C. D. Ferris and S. H. Snyder, *Annu. Rev. Physiol.* **54**, 469 (1992).
6. Albino oocytes (Dumont stage V) were prepared as reported (*3*) except that the incubation medium was supplemented with horse serum (5%) [M. W. Quick, J. Naeve, N. Davidson, H. A. Lester, *BioTechniques* **13**, 360 (1992)]. Serum-free solutions were used to wash the oocytes at least 6 hours before study. For experiments with exogenous receptors, 5 ng of m3AChR cRNA (in vitro transcript from a cDNA clone) was injected as a 47-nl bolus 48 hours before experimentation, and the oocytes were incubated at 19°C. From 30 to 240 min before imaging, 47 nl of Calcium Green (0.25 mM) was injected, which resulted in a final concentration of ~12 μM, assuming a 1-μl volume of distribution.
7. A Lasersharp Bio-Rad MRC-600 box adapted to a Zeiss IM35 inverted microscope was used with an Olympus DPlanApo ×10 ultraviolet objective (0.4 numerical aperture) for confocal imaging [C. Bliton, J. Lechleiter, D. E. Clapham, *J. Microsc.* **169**, 15 (1993). Excitation provided by the 488-nm line of a 25-mW argon laser was filtered to less than 5% transmission by neutral density filters (Omega Optical). Returning fluorescence was long pass–filtered (515 nm) and detected with the confocal aperture set to its maximal opening (7 mm) in the low signal mode.
8. The digitized images were stored on optical disk and studied with ANALYZE software (Mayo Foundation, Rochester, MN) on a Silicon Graphics Personal Iris Computer.
9. A 10-mm square patch of woven mesh (Spectrum, 750-μm spacing) was attached with silicon rubber to a cover slip that functioned as the bottom of a 2-ml chamber. The mesh improved the kinetics of the ACh response about fourfold by allowing ACh better access to the space between the oocyte and the cover slip. Solution changes by addition of 750 μl to the bath (initial volume = 750 μl) were considered complete within 10 s. The extracellular solution with a low concentration of Ca^{2+} contained 96 mM NaCl, 5 mM $MgCl_2$, 2 mM KCl, 5 mM Hepes (pH 7.5), and 0.1 mM EGTA (free Ca^{2+} ~10 nM). EGTA was replaced with $CaCl_2$ to obtain the desired final concentration of extracellular Ca^{2+}. A conventional two-electrode voltage clamp technique was used in parallel with imaging. Oscillations in the Ca^{2+}-activated $I_{Cl,Ca}$ reflected the full-field average concentration of Ca^{2+} and are not shown. Experiments were conducted at 22° to 25°C (S. Girard and D. E. Clapham, *Methods Cell Biol.*, in press).
10. Calcium Green-1 (Molecular Probes, Eugene, OR) has a dissociation constant (K_d) for Ca^{2+} of 189 nM in 100 mM KCl at 22°C.
11. J. Lechleiter, S. Girard, D. Clapham, E. Peralta, *Nature* **350**, 505 (1991).
12. I. Parker and R. Miledi, *Proc. R. Soc. London Ser. B* **231**, 27 (1987). The activation of native muscarinic receptors has been shown to trigger the influx of extracellular Ca^{2+} that is insensitive to nifedipine (50 μM) [M. Lupu-Meiri, H. Shapira, Y. Oron, *FEBS Lett.* **262**, 165 (1990)]. In these experiments, Ca^{2+}-activated $I_{Cl,Ca}$ was used as the assay for cytosolic Ca^{2+}. Depolarization to 0 mV blocks the influx of extracellular Ca^{2+}, which suggests that voltage-activated Ca^{2+} currents are minor or that they inactivate during prolonged depolarization [R. Miledi, *Proc. R. Soc. London Ser. B* **215**, 491 (1982); M. E. Barish, *J. Physiol. (London)* **342**, 309 (1983)].
13. The time constant of inhibition of the Ca^{2+}-activated $I_{Cl,Ca}$ by atropine (200 μM) was less than 8 s in four m3AChR-expressing oocytes that exhibited oscillations induced by ACh (1 μM).
14. One possible Ca^{2+} influx pathway is related to depletion of stores by unknown second messengers [J. W. Putney, Jr., in *Advances in Second Messenger and Phosphoprotein Research*, J. W. Putney, Jr., Ed. (Raven, New York, 1992), pp. 143–160; M. Hoth and R. Penner, *Nature* **355**, 353 (1992); R. Penner, G. Matthews, E. Neher, *ibid.*

334, 499 (1988); J. W. Putney, Jr., *Cell Calcium* 11, 611 (1990); G. St J. Bird *et al.*, *Nature* 352, 162 (1991)]. Attempts to deplete the Ca^{2+} stores with two blockers of the microsomal Ca^{2+} adenosine triphosphatase, thapsigargin [Y. Kijima, E. Ogunbunmi, S. Fleischer, *J. Biol. Chem.* 266, 22912 (1991); O. Thastrup, P. J. Cullen, B. K. Drobak, M. R. Hanley, *Proc. Natl. Acad. Sci. U.S.A.* 87, 2466 (1990)] and 2,5-di-(*tert*-butyl)-1,4-benzohydroquinone [G. A. Moore, D. J. McConkey, G. E. N. Kass, P. J. O'Brien, S. Orrenius, *FEBS Lett.* 224, 331 (1987)], applied at extracellular concentrations of 20 μM for 10 min were unsuccessful (n = 10). Hydrophobic, membrane-permeant drugs are probably absorbed by the lipophilic yolk platelets [J. N. Dumont, *J. Morphol.* 136, 153 (1972); W. M. Bement and D. G. Capco, *J. Electron Microsc. Tech.* 16, 202 (1990)]. Therefore, it remains uncertain whether depletion of the IP_3-sensitive Ca^{2+} store itself is a sufficient trigger for Ca^{2+} influx in *Xenopus* oocytes.

15. S. DeLisle, K. H. Krause, G. Denning, B. V. L. Potter, M. J. Welsh, *J. Biol. Chem.* 265, 11726 (1990). IP_3S_3 has high affinity for the IP_3R of the cerebellum (K_d = 31 ± 3 nM) and a median effective concentration (EC_{50}) for Ca^{2+} release of ~5 μM in permeabilized Swiss 3T3 cells. In *Xenopus* oocytes, IP_3 was five to ten times more potent than IP_3S_3 in generating oscillations in $I_{Cl,Ca}$. Heparin antagonized both the IP_3S_3-induced waves and the binding of IP_3 to oocyte microsomes [the amount required for 50% inhibition (IC_{50}) = 2 μg/ml)] (*6–9, 13*) [B. V. L. Potter, R. A. J. Challis, S. R. Nahorski, *Du Pont Biotech. Update* 5, 1 (1990); C. W. Taylor, M. J. Berridge, K. D. Brown, A. M. Cooke, B. V. L. Potter, *Biochem. Biophys. Res. Commun.* 150, 626 (1988); J. E. Ferguson, B. Potter, R. Nuccitelli, *ibid.* 172, 229 (1990)].
16. Inositol 1,4,5-triphosphate, inositol 2,4,5-triphosphate, and inositol 1,3,4-triphosphate have been shown to induce Ca^{2+} influx in *Xenopus* oocytes. In these experiments, the Mn^{2+} block of $I_{Cl,Ca}$ was used to assay changes in cytosolic Ca^{2+} [S. DeLisle, D. Pittet, B. V. L. Potter, P. D. Lew, M. J. Welsh, *Am. J. Physiol.* 262, C1456 (1992); P. M. Snyder, K. H. Krause, M. J. Welsh, *J. Biol. Chem.* 263, 11048 (1988)].
17. Manganese has been used as an indicator of Ca^{2+} influx because it quenches indol-1 and fura-2 (Molecular Probes, Eugene, OR) fluorescence [G. Grynkiewicz, M. Poenie, R. Tsien, *J. Biol. Chem.* 260, 3440 (1985)]. We found in some cases that extracellular Mn^{2+} (1 to 10 mM) irreversibly increased the Calcium Green signal in IP_3S_3-stimulated oocytes, which suggests that Mn^{2+} enhances Calcium Green fluorescence and that the influx pathway is at least partially permeable to Mn^{2+}. This makes it unsuitable as an influx channel antagonist in simultaneous imaging and electrophysiological experiments. Conversely, 1 mM La^{3+} reliably blocked influx in eight of eight oocytes without affecting the ability of the indicator to respond to Ca^{2+}. In the absence of extracellular Ca^{2+}, the application of La^{3+} did not influence the Ca^{2+} waves induced by IP_3S_3 (5 μM).
18. I. Parker and I. Ivorra, *Proc. Natl. Acad. Sci. U.S.A.* 87, 260 (1990).
19. J. B. Parys *et al.*, *J. Biol. Chem.* 267, 18776 (1992). A bell-shaped dependence of IP_3-mediated Ca^{2+} release on free cytosolic Ca^{2+} has also been observed in smooth muscle and rat cerebellar microsomes and in IP_3R channels isolated from rat cerebellum and reconstituted into lipid bilayers [M. Iino, *J. Gen. Physiol.* 95, 1103 (1990); E. A. Finch, T. J. Turner, S. M. Goldin, *Science* 252, 443 (1991); I. Bezprozvanny, J. Watras, B. E. Ehrlich, *Nature* 351, 751 (1991)].
20. N. L. Allbritton, T. Meyer, L. Stryer, *Science* 258, 1812 (1992).
21. We observed regenerative Ca^{2+} waves for up to 7 min in the absence of extracellular Ca^{2+} after injection of IP_3S_3 (100 μM) in 12 of 16 oocytes.
22. Because Calcium Green does not shift its emission or excitation spectrum upon binding Ca^{2+}, ratiometric measurement of Ca^{2+} was not possible. Previous measurements set the resting Ca^{2+} concentration in oocytes at ~100 nM (*3, 6–9*). Comparison of Calcium Green with dextran-bound Calcium Green indicates that, at the concentrations used, the dye is not a significant mobile Ca^{2+} buffer and does not alter our observations.
23. We thank M. Berridge for comments on the work, D. Skuldt and J. Amundson for assistance, A. Lückhoff for programming, the ANALYZE software group (Mayo Foundation), E. Peralta for the m3AChR plasmid, and K. Hedin and L. Stehno-Bittel for critical review of the manuscript. Supported by the NIH, the Whitaker Foundation, Glaxo Inc., and the J. W. Kieckhefer Foundation. D.C. is an Established Investigator of the American Heart Association.

23 October 1992; accepted 26 January 1993

Force of Single Kinesin Molecules Measured with Optical Tweezers

Scot C. Kuo* and Michael P. Sheetz

Isometric forces generated by single molecules of the mechanochemical enzyme kinesin were measured with a laser-induced, single-beam optical gradient trap, also known as optical tweezers. For the microspheres used in this study, the optical tweezers was spring-like for a radius of 100 nanometers and had a maximum force region at a radius of ~150 nanometers. With the use of biotinylated microtubules and special streptavidin-coated latex microspheres as handles, microtubule translocation by single squid kinesin molecules was reversibly stalled. The stalled microtubules escaped optical trapping forces of 1.9 ± 0.4 piconewtons. The ability to measure force parameters of single macromolecules now allows direct testing of molecular models for contractility.

Biological forces in motile systems, such as those involving ciliary dynein and actomyosin, are usually studied as the sum of contributions from many force-generating units (*1*). However, the mechanochemical enzyme kinesin can function as an individual molecule. Kinesin that is adsorbed to glass moves microtubules so that they pivot around a single attachment point (*2*). The concentration dependence of the motility, calculated as an effective Hill coefficient of 1 for kinesin adsorbed to glass cover slips (*2*) or as a Poisson distribution for kinesin adsorbed to glass beads (*3*), indicates that one molecule alone can generate force and move microtubules. We have directly measured the force generated by an individual kinesin molecule using the single-beam optical gradient trap, also known as optical tweezers (*4*).

To characterize the optical trap, we used viscous drag to displace trapped microspheres that were 0.55 μm in diameter. All calibration experiments were performed at least 2 μm from the cover slip surface to minimize viscous coupling to the glass surface, so deviations from Stokes drag were <7% (*5*). For all biological force measurements, we calibrated the escape force (F_{esc}) from the optical tweezers by using a laminar flow cell (*6*). However, optical forces during escape from the optical tweezers are spatially complex, requiring nanometer-level characterization of the optical trap to interpret subsequent experiments. Such characterization would be biased by the shear gradient of the flow cell, so we used viscous forces that were generated by moving the microscope specimen with a piezoceramic-driven stage (*7*). The stage had a maximal usable velocity of ~150 μm s^{-1} (~0.8 pN of viscous drag), making it less appropriate for direct calibration of biological force measurements. Trapped particles were alternately displaced by the piezoceramic stage moving at constant velocity, and their positions were monitored while laser irradiation was reduced (Fig. 1A). Normalized to the laser irradiation at the specimen, a force and displacement profile can be constructed (Fig. 1B). Force is proportional to the displacement for the first ~100 nm. This force-displacement profile qualitatively agrees with theoretical models of the optical trap (*8*). Because of video limitations, the region of maximum force has not been precisely determined, but it appears to be located at a radius of 150 ± 26 nm (SD) (Fig. 1C).

Optical forces were applied to streptavidin-coated latex microspheres that were attached as handles to biotinylated microtubules. The biotinylation procedure, both with and without the attachment of microspheres, did not alter kinesin-driven gliding velocities of the microtubules. After evaluating different procedures for constructing biotin-specific beads (*9*), we covalently attached bovine serum albumin to carbodiim-

Department of Cell Biology, Duke University Medical Center, Durham, NC 27710.

*To whom correspondence should be addressed at the Department of Biomedical Engineering, Johns Hopkins University Medical School, Baltimore, MD 21205.